# Pseudorabies Virus Infection Accelerates Degradation of the Kinesin-3 Motor KIF1A

Running Title: Pseudorabies Virus Accelerates KIF1A Degradation

Hao Huang[a], Orkide O. Koyuncu[a], and Lynn W. Enquist[a#].

[a]Department of Molecular Biology, Princeton University, Princeton, New Jersey, USA

[#]Corresponding author: Lynn W. Enquist, lenquist@princeton.edu

Word Count: Abstract (231),

Main Text (5744)

Keywords: alphaherpesvirus, pseudorabies virus, kinesin, KIF1A, proteasomal degradation, axonal sorting.

## Abstract

Alphaherpesviruses, including pseudorabies virus (PRV), are neuroinvasive pathogens that establish life-long latency in peripheral ganglia following the initial infection at mucosal surfaces. The establishment of latent infection and the subsequent reactivations during which newly-assembled virions are sorted into and transported anterogradely inside axons to the initial mucosal site of infection, rely on axonal bidirectional transport mediated by microtubule-based motors. Previous studies using cultured peripheral nervous system (PNS) neurons have demonstrated that KIF1A, a kinesin-3 motor, mediates the efficient axonal sorting and transport of newly-assembled PRV virions. In this study, we report that KIF1A, unlike other axonal kinesins, is an intrinsically unstable protein prone to proteasomal degradation. Interestingly, PRV infection of neuronal cells leads not only to a non-specific depletion of KIF1A mRNA, but also to an accelerated proteasomal degradation of KIF1A proteins, leading to a near depletion of KIF1A protein late in infection. Using a series of PRV mutants deficient in axonal sorting and anterograde spread, we identified the PRV US9/gE/gI protein complex as a viral factor facilitating the proteasomal degradation of KIF1A proteins. Moreover, by using compartmented neuronal cultures that fluidically and physically separate axons from cell bodies, we found that the proteasomal degradation of KIF1A occurs in axons during infection. We propose that PRV anterograde sorting complex, gE/gI/US9, recruits KIF1A to viral transport vesicles for axonal sorting and transport, and eventually accelerates the proteasomal degradation of KIF1A in axons.

## Importance

Pseudorabies virus (PRV) is an alphaherpesvirus related to human pathogens herpes simplex virus -1, -2 and varicella zoster virus. Alphaherpesviruses are neuroinvasive pathogens that establish life-long latent infections in the host peripheral nervous system (PNS). Following reactivation from latency, infection spreads from the PNS back via axons to the peripheral mucosal tissues, a process mediated by kinesin motors. Here, we unveil and characterize the underlying mechanisms for a PRV-induced, accelerated degradation of KIF1A, a kinesin-3 motor promoting the sorting and transport of PRV virions in axons. We show that PRV infection disrupts the synthesis of KIF1A, and simultaneously promotes the degradation of intrinsically unstable KIF1A proteins by proteasomes in axons. Our work implies that the timing of motor reduction after reactivation would be critical because progeny particles would have a limited time window for sorting into and transport in axons for further host-to-host spread.

## Introduction

Alphaherpesviruses, including human pathogens herpes simplex virus-1 and -2, varicella-zoster virus, and the veterinary pathogen pseudorabies virus (PRV), are neuroinvasive pathogens that establish and maintain life-long latency in the sensory and automatic ganglia of the peripheral nervous system (PNS) of their mammalian hosts following initial infection at mucosal surfaces (1-3). Latently infected neurons in peripheral ganglia undergo occasional reactivation, during which viral genomes are actively replicated and new viral particles assembled. Spread of infection to new hosts requires that these progeny virions be transported to the initial site of epithelial infection, where replication and subsequent host-to-host transmission occur. On rare occasions, infection spreads from the PNS to the central nervous system, often with serious consequences such as herpes simplex encephalitis (HSE).

Axonal bidirectional transport mechanisms are crucial for the virions and virus proteins to move efficiently through the PNS axons, which are often centimeters to meters long (4). In uninfected neurons, microtubule-based motors, including minus-ended directed cytoplasmic dynein and plus-ended directed kinesin superfamily motors, mediate fast axonal transport of RNAs, proteins, organelles, and vesicles between cell bodies and axonal termini for the maintenance and proper functioning of axons (5, 6). Neuroinvasive viruses such as the alphaherpesviruses and rabies virus have evolved to adopt existing axonal transport machinery for efficient neuroinvasion and subsequent spread to new hosts. A notable example is rabies virus (RABV), whose phosphoprotein (P) binds to LC8 dynein light chain, and was shown to hijack the P75NTR-dependent transport to facilitate fast retrograde axonal transport in sensory DRG neurons (7).

Initially after infection of peripheral tissues, alphaherpesvirus virions bind to PNS axon terminals, and viral capsids are released into axons where they recruit cytoplasmic dynein, via inner tegument proteins UL36 and UL37 (8, 9). This complex then moves in the MT minus-end direction towards the cell body and deposits the viral DNA inside the nucleus. After reactivation of a latent PNS infection, kinesin-superfamily motors are recruited both for viral egress at cell bodies, as well as for sorting into axons and subsequent transport of viral structural proteins and newly-assembled virions (10-14). Previous studies in sympathetic PNS neurons revealed that a subpopulation of fully-enveloped PRV virions in transport vesicles recruit KIF1A, a kinesin-3 motor, through the interactions with a gE/gI/US9 tripartite membrane protein complex in lipid rafts at late Golgi network compartments (e.g., late endosomes or the trans-Golgi network (TGN)) (14, 15). After this interaction, fully enveloped virions in transport vesicles are sorted into axons followed by unidirectional anterograde transport before egressing along the axonal shaft (16). In PRV infected neurons, ectopic expression of dominant-negative KIF1A proteins significantly reduced the number of PRV particles transported in the anterograde direction, demonstrating the critical role of KIF1A in sorting virus particles into axons and also in subsequent transport (14). In this report, we focus on a curious observation made by Kramer et al, who noted that the amount of KIF1A in infected cultured neuronal cells decreased significantly late after PRV infection (14).

In uninfected neurons, the kinesin motor KIF1A mediates fast axonal transport of membranous vesicles including synaptic vesicle precursors and dense core vesicles, and is critical in dendrite morphogenesis and synaptogenesis (17-19). Neurons lacking KIF1A showed impaired transport in synaptic vesicle precursors, marked neuronal degeneration, and death in both cultured neurons

and *in vivo* (20). Despite its functional importance, several lines of evidence suggest that KIF1A motors are degraded upon the completion of their axonal transportation runs, and are not recycled for further use. Studies with a ligature applied to the mouse sciatic nerve revealed increased antibody staining of KIF1A in the proximal (close to the cell body), but not distal (close to the axonal terminal), region of ligature, suggesting that once KIF1A motors entered axons, they did not return to the cell bodies (e.g. with dyneins) (21). UNC-104, the KIF1A homolog in *C. elegans,* was shown to be degraded by ubiquitin-related pathways at synapses of mechanosensory neurons (22). More importantly, the stability of UNC-104 protein strongly correlates with the motor's specific binding to cargo, implying a potential mechanistic link between motor degradation and cargo release (22).

In this study, we investigated KIF1A protein dynamics during PRV infection both in neuronal cell lines and in primary neurons. Here, we report that KIF1A (kinesin-3), unlike kinesin-1 and kinesin-2 motors, is intrinsically prone to proteasomal degradation in uninfected neuronal cells. We further showed that PRV infection blocks new synthesis of this motor, and that viral anterograde-sorting complex US9/gE/gI specifically targets KIF1A for proteasomal degradation, resulting in a near depletion of the protein in 24 hours following infection. Using compartmented neuronal cultures that fluidically and physically separate axons from cell bodies, we found that the proteasomal degradation of KIF1A proteins occurs in axons. Moreover, using a series of PRV mutants deficient in anterograde spread, and using adenovirus vectors to express the viral proteins in neuronal cells, we discovered that the PRV US9/gE/gI protein complex targets specifically KIF1A motors for proteasomal degradation. Altogether, these results suggest that progeny PRV particles recruit KIF1A motors for efficient axonal sorting and anterograde transport that leads to the degradation

of the motor protein in axons. Since new synthesis of KIF1A is also blocked by PRV infection, these results suggest progeny particles have a limited time window for sorting into and transport in axons for further host-to-host spread.

## Results

### In uninfected, differentiated PC12 cells, the steady state concentration of KIF1A protein is achieved through rapid protein synthesis and proteasomal degradation.

We tested the hypothesis that in differentiated PC12 cells axonal kinesins undergo rapid degradation while protein synthesis continues. To determine the role of the proteasome in this process, we treated uninfected differentiated PC12 cells with the proteasomal inhibitor MG132 for 2, 4, 6, and 8 hours, and monitored the protein concentration of three different kinesin motors: KIF5 (kinesin-1, and the conventional kinesin), KIF3A (kinesin-2), and KIF1A (kinesin-3). MG132 treatment led to more than a 2-fold increase in KIF1A concentration within 6 hours post treatment, indicating that KIF1A protein rapidly accumulated upon proteasome inhibition (Figure 1A and B). However, this surge in KIF1A concentration was ablated when PC12 cells were simultaneously treated with MG132 and cycloheximide, a protein synthesis inhibitor, and KIF1A concentration remained at the similar levels as in untreated cells. These experiments demonstrated that KIF1A proteins are degraded by the proteasomes with new proteins efficiently made to maintain protein steady state levels. Consistent with this idea, in cells treated with CHX alone, KIF1A concentration dropped by over 50% within 4 hours of treatment (Figure 1A and B).

In contrast to KIF1A, neither KIF5 nor KIF3A protein concentration increased significantly during MG132 treatment (Figure 1A, C and D). With both MG132 and CHX treatments, KIF5 and KIF3A concentrations appeared unchanged in the 8 h treatment period (Figure 1A, C and D), suggesting that while both proteins are degraded by proteasomes, their rate of degradation is much slower than that of KIF1A. As a result, the half-lives of both KIF5 and KIF3A proteins were much longer (> 8 hours) than the half-life of KIF1A in CHX-treated PC12 cells.

**PRV infection induces specific reduction of KIF1A protein late in infection**

The inherent instability of KIF1A in uninfected cells prompted us to explore an observation previously made in our laboratory: the concentration of KIF1A protein, the major kinesin facilitating axonal sorting and transport of PRV virions, decreased late in PRV infection of sympathetic neuronal cells. This observation might explain the significant numbers of immobile PRV particles in axons late in infection (23). Accordingly, we infected differentiated PC12 cells with PRV Becker at an MOI of 20 for 3, 8, 12, 16, 20, and 24 hours, and monitored KIF1A protein levels by quantitative western blot methods. Similar to the previous report, we found that the KIF1A protein concentration dropped by ~90% at 24 hpi (Figure 2A and B, Figure S1). To determine if PRV infection affects the steady state concentrations of other kinesin motors, we monitored the protein levels of KIF5 and KIF3A, two kinesins well-characterized in mediating axonal transport. Neither KIF5 nor KIF3A protein levels were affected by PRV infection (Figure 2).

**PRV infection reduces both KIF1A and KIF5B transcripts.**

Alphaherpesviruses promote the instability of many host cell transcripts early in infection, leading to reduced protein synthesis (24-27). We hypothesized that the loss of KIF1A proteins in PRV-infected PC12 cells resulted from such mRNA degradation. We therefore measured the amounts of KIF1A transcripts in PRV infected cells by qRT-PCR. Differentiated PC12 cells were infected with PRV Becker and the attenuated vaccine strain PRV Bartha at an MOI of 20 for 3, 8, 12, 16, 20, 24 hours. Infected cells were collected for RNA extraction and qRT-PCR analysis of KIF1A, KIF5B, and GAPDH mRNA level (Figure 3). In PRV Becker-infected cells, we detected a significant and uniform reduction of KIF1A, KIF5B, and GAPDH transcripts as early as 8 hpi, and their respective concentrations dropped by more than 80% at 16 hpi (Figure 3A).

Compared to PRV Becker infection, PRV Bartha infection decreased KIF1A transcripts at a slower rate, starting at 12 hpi, with more than 80% loss at 20 hpi (Figure 3B). Reduction of GAPDH and KIF5B transcripts occurred with comparable rates and magnitude to the KIF1A transcripts. These experiments showed that KIF1A transcripts were reduced in PRV-infected PC12 cells, but with different kinetics after infection by different PRV strains. Such transcriptional regulation may be one reason why KIF1A protein levels drop significantly during PRV infection. However, this effect was not specific for KIF1A, because KIF5B transcripts were also reduced after infection. Therefore, the specific loss of KIF1A and not KIF5B proteins in infected neurons is not due to reduction of transcript levels.

**KIF1A is degraded by the proteasome during PRV infection in differentiated PC12 cells and in primary SCG neurons.**

We found that KIF1A (but not other kinesins) is rapidly degraded by the proteasome in uninfected PC12 cells. We also knew from previous studies that complexes of PRV US9 and KIF1A contain the E3-ubiquitin ligases NEDD4 and EP0, suggesting that KIF1A may be degraded via the ubiquitin-proteasome pathway after PRV infection (14). To examine this possibility, we infected differentiated PC12 cells with PRV Becker at an MOI of 20, followed by treatment with the proteasomal inhibitor MG132 at 12 hpi. In mock-infected cells, KIF1A proteins accumulated rapidly, doubling the concentration in 8 hours, after MG132 treatment (Figure 4A and C). However, in PRV Becker infected cells, MG132 treatment led to an effective stabilization of KIF1A protein levels where the protein concentration remained mostly unchanged during the treatment period (Figure 4B and C). This finding suggests that, in the late phase of infection, new KIF1A synthesis is blocked but proteasomal degradation continues, leading to the accelerated loss of KIF1A during PRV infection.

These studies were done in differentiated PC12 cells that have similar attributes to sympathetic neurons. We performed similar experiments in primary rat superior cervical ganglionic neurons (SCG) cultured in compartmented chambers where we could examine kinesin motor concentration in isolated axons. We cultured primary sympathetic rat SCG neurons in trichambers, in which axons (in the neurite compartment, N) were fluidically and physically separated from cell bodies (in the soma compartment, S) (Figure 5A). SCG cell bodies in the S compartment were infected with PRV Becker for 24 hours and extracts from the S and N compartments were collected for western blot analysis. The concentration of KIF1A protein decreased dramatically both in cell bodies and axons after PRV infection (Figure 5B).

We further determined if the loss of KIF1A protein is mediated by proteasomes in isolated SCG axons during infection. SCG neurons cultured in trichambers were infected with PRV Becker in the S compartment, followed by MG132 treatment in the N compartment at 8 hpi. KIF1A protein levels were reduced significantly in both S and N compartments after PRV Becker infection (Figure 5C). Moreover, axonal KIF1A levels were partially restored by MG132 treatment in the N-compartment (Figure 5C). We concluded that PRV infection accelerates the degradation of KIF1A proteins by proteasomes in axons.

**Expression of both PRV early and late genes are involved in accelerated KIF1A degradation during infection.**

We next searched for viral proteins that might accelerate KIF1A protein degradation. First, we determined if early events such as virion entry and tegument protein delivery would be enough to promote KIF1A degradation. We infected PC12 cells either with UV treated PRV Becker virions (UVPRV) or with a PRV mutant that lacks IE180 (PRV HKO146), the single master immediate early transcriptional activator of viral genes required for RNA transcription and DNA replication (28, 29). Both UVPRV and PRV HKO146 (grown in IE180-complementing cells) enter the cells, release outer tegument proteins (including vhs, the virion host shutoff protein), and deposit viral DNA in the nucleus, but neither can initiate *de novo* viral protein synthesis. We found that after either infection, KIF1A was not degraded (Figure 6A). We concluded that PRV entry into PC12 cells is not sufficient to accelerate KIF1A protein degradation.

We next determined if PRV immediate-early and early, or late genes were involved in KIF1A protein degradation. We pretreated differentiated PC12 cells with the herpesvirus DNA replication inhibitor AraT for 15 minutes, and infected them with PRV Becker for 8, 12, 16, 20, 24 hours. AraT inhibition should have minimal effects on early viral gene expression, but should severely diminish late gene expression. As expected, we detected comparable amounts of the early protein, EP0, in both AraT treated and untreated cells during infection, whereas the accumulation of the late protein VP5 (also major capsid protein, MCP) was severely affected by the AraT treatment (Figure 6B). AraT treatment led to a minor, though statistically significant, stabilization of KIF1A protein in the later stage of infection (Figure 6B-C). This experiment demonstrated that while PRV IE and/or E gene products could promote a reduction in KIF1A protein levels (e.g. potentially through the reduction of KIF1A transcripts), viral proteins accumulating in the late phase of infection are also required for efficient degradation of KIF1A.

**PRV anterograde-sorting complex US9/gE/gI promotes the accelerated degradation of KIF1A proteins.**

PRV particles in transport vesicles use KIF1A for sorting into axons and subsequent transport. The recruitment of KIF1A to transport vesicles containing enveloped PRV particles at the TGN requires viral membrane protein US9. This interaction is stabilized by the heterodimer of gE/gI. We had noted previously that two ubiquitin ligases, NEDD4 and viral EP0, co-purified with US9 and KIF1A (14). Since KIF1A instability results from proteasomal degradation, we hypothesized that the tripartite complex US9/gE/gI might be involved in accelerating KIF1A degradation. We infected differentiated PC12 cells with PRV Becker and two PRV mutants that were deleted for

US9, gE, and gI genes, and are deficient in axonal sorting and anterograde spread: PRV Bartha and PRV BaBe (PRV Becker with the Us region of Bartha). Infection with either mutant lacking US9, gE, and gI partially restored KIF1A proteins during PRV infection (Figure 7A and B). As both of these mutant viruses degrade host transcripts presumably through early proteins, KIF1A levels show a comparable decrease between 8-12 hpi to Becker infection. However, we did not detect the rapid decrease in KIF1A protein levels after 12 h in Bartha and BaBe infections, suggesting that the tripartite complex help accelerate the degradation of KIF1A by proteasomes (Figure 1A and B). We further infected PC12 cells with two PRV US9 mutants deficient in anterograde spread, PRV 161 (US9-null), and PRV 172 (Y49-50A US9, functionally null). In PRV172 infections, all US9, gE, and gI proteins were present, but the dityrosine mutation within the acidic cluster of US9 gene disrupted the formation of the tripartite complex, and made the virus particles incapable of recruiting KIF1A and anterograde spread (14, 30, 31). Both PRV 161 and PRV 172 infections restored KIF1A proteins in magnitudes comparable to infections with PRV Bartha and Babe (Figure 7A and B). These results suggested that the formation of the tripartite complex is necessary for the accelerated loss of KIF1A proteins.

We further determined if the US9/gE/gI complex could target KIF1A for degradation independent of PRV infection. We transduced differentiated PC12 cells with adenovirus vectors expressing the US9, gE, and gI protein, either individually or in combination, for 1, 2, 3, 4, 5 days. Neither the control Ad-GFP nor Ad-GFP-US9 transduction resulted in KIF1A protein instability, but when PC12 cells were transduced with equal units of the three adenovirus vectors expressing US9, gE, and gI, the KIF1A protein was completely degraded by 5 days post transduction (Figure 7C and

Figure S2). We concluded that a functional anterograde sorting complex could augment the proteasomal degradation of KIF1A protein independent of infection by PRV.

Altogether these results suggest that PRV infection leads to the depletion of KIF1A proteins in infected neurons both by blocking new protein synthesis and also specifically targeting the motor for anterograde spread of progeny late in infection, which eventually accelerates proteasomal degradation of KIF1A.

## Discussion

A major distinction of alphaherpesviruses from most of other neuroinvasive viruses is their ability to travel in both anterograde and retrograde directions in axons and in neuronal circuits (4). The anterograde transport of newly assembled herpesvirus virions is crucial for the viral life cycle because it ensures that virus particles are sorted into axons to facilitate inter-host transmission. KIF1A mediates the sorting and transport of PRV egressing virions in axons, with the dynamics of transport involving long segment runs with high velocity (Vmax ~2.4μm/s) (16). The anterograde transport of PRV virions was greatly hindered in the neurons expressing the dominant-negative form of KIF1A protein (14). In this study, we demonstrated that KIF1A is intrinsically prone to degradation by the proteasomes, and that PRV infection accelerates such degradation and results in near depletion late in infection. The steady state concentration of KIF1A protein in uninfected neuronal cells is achieved through rapid protein synthesis and proteasomal degradation. Upon PRV infection, KIF1A mRNA was degraded in a nonspecific manner, reducing KIF1A protein synthesis while the existing proteins were gradually degraded by the proteasome. In addition, adenovirus vectors expressing proteins constituting the PRV anterograde sorting

299 complex US9/gE/gI induced a decline in KIF1A protein level independent of PRV infection,
300 suggesting the US9/gE/gI tripartite complex accelerates the proteasomal degradation of KIF1A
301 and contributes, alongside PRV host shutoff, to the decline in KIF1A protein during PRV infection.
302 Importantly, using compartmented primary neuron cultures we showed that proteasomal
303 degradation of KIF1A is accelerated in axons after PRV infection.
304
305 **The intrinsic instability of the KIF1A protein.**
306
307 The kinesin motor KIF1A mediates fast axonal transport of membranous vesicles including
308 synaptic vesicle precursors and dense core vesicles, and is critical in synaptogenesis (17, 18). In
309 differentiated PC12 cells, KIF1A protein levels decreased rapidly upon treatment with the protein
310 synthesis inhibitor cycloheximide (CHX), and showed an apparent half-life of approximately 4
311 hours. The half-lives of kinesin-1 and -2 motors were longer under the same condition (>8 hours).
312 Our results are consistent with a previous proteomics study using rat cortical neurons, where
313 KIF1A had the 8$^{th}$ shortest half-life in among ~2800 proteins measured ($t_{1/2}$ = 0.42 day) (32),
314 suggesting that this is a consistent characteristic of KIF1A in both CNS and PNS neurons. The
315 decline in KIF1A concentration is blocked when PC12 cells were treated simultaneously with
316 CHX and MG132, demonstrating that the loss of KIF1A protein was predominately mediated by
317 proteasomes. Our results confirmed another previous proteomics study where the half-life of the
318 KIF1A protein increased and the degradation rate dropped upon inhibition of proteasomes (33).
319
320 UNC-104, the KIF1A homolog in *C. elegans*, was shown to be degraded at synapse regions *in vivo*
321 in an ubiquitin-dependent manner. Moreover, the stability of the motor was linked to its capacity

for cargo binding (22). It was also proposed that the degradation of Liprinα1, an cargo adaptor for KIF1A, by either proteasome or CaMKII phosphorylation was required for the "unloading" of LAR (leukocyte common antigen- related) family of receptor protein tyrosine phosphatases at synapses (34, 35). These studies imply a potential mechanistic link between motor degradation and cargo release. Since we also observed proteasomal degradation of KIF1A in fluidically and physically separated axons during PRV infection, KIF1A may be actively degraded in axons by proteasomes upon release of viral cargo.

The relative stabilities of KIF5 and KIF3A proteins were unexpected, since several lines of evidence suggested that both motors are actively degraded in axons (36-39). However, unlike KIF1A, both KIF5 and KIF3A also mediate short distance transport of cellular cargoes within cell bodies, and may be recycled for future use. The particular short half-life of KIF1A is consistent with the idea that KIF1A is a specialized motor for axonal transport.

**The reduction of KIF1A mRNA upon PRV infection.**

The dynamic steady state level of KIF1A protein in uninfected cells suggests that, in PRV-infected cells, KIF1A protein concentration may be sensitive to viral host shutoff or mRNA instability induced by infection. Alphaherpesviruses reduce/block the synthesis of some cellular proteins after infection to facilitate viral gene expression and to evade host antiviral responses. The virion host shutoff protein (vhs) is an endoribonuclease encoded by the viral UL41 gene (40-42). HSV-1 vhs enters the infected cells as a part of incoming virion tegument, and subsequently interacts with translation initiation factors eIF4H, eIF4B, and eIF4A to degrade host mRNAs and halts host

345 protein translation (43, 44). Infection of PC12 cells with inactivated virions (UV'd, IE180-null
346 PRV) did not lead to the decline in KIF1A protein. We conclude that tegument proteins like vhs
347 delivered by entering particles are not sufficient for the reduction in KIF1A protein during
348 infection.
349
350 We further analyzed the accumulation of cellular mRNAs during infection and compared the levels
351 of kinesin motor transcripts. qRT-PCR analysis of PRV-infected PC12 cells revealed that the
352 levels of KIF1A, KIF5B, and GAPDH transcripts all decreased significantly at similar rates,
353 starting as early as 3 h.p.i., and reaching almost full depletion at 12 h.p.i. The reduction of KIF1A
354 mRNA reduced the rate of new protein synthesis. This reduction of new KIF1A proteins, coupled
355 with the active degradation of existing KIF1A motors by proteasomes, leads to the significant
356 decrease in KIF1A protein concentration in infected neuronal cells.
357
358 **The PRV anterograde sorting complex US9/gE/gI directs more KIF1A motors to be**
359 **degraded by proteasomes.**
360
361 US9 forms a complex with two other membrane proteins, gE and gI to sort progeny PRV virions
362 in transport vesicles into axons (14, 15)(J. Scherer, I. B. Hogue, Z. A. Yaffe, N. S. Tanneti, B. Y.
363 Winer, M. Vershinin, L. W. Enquist, submitted for publication). We have previously identified
364 KIF1A as an interaction partner of PRV US9 protein (14). In addition, we had noted that two
365 ubiquitin ligases, NEDD4 and viral EP0, co-purified with US9 and KIF1A (14). Since we also
366 showed accelerated proteasomal degradation of KIF1A during infection, we hypothesized that the
367 PRV anterograde sorting complex, gE/gI/US9, could independently recruit KIF1A to viral

transport vesicles for axonal sorting and transport, and eventually promote the proteasomal degradation of KIF1A in axons. We investigated this hypothesis using adenovirus vectors to express the components of the anterograde sorting complex (one by one and in combination) in neuronal cells without PRV infection. In cells transduced with adenovirus vectors expressing US9, gE, and gI, US9 interacts with the gE/gI heterodimer in lipid rafts, and the US9, gE, and gI complex was observed to undergo axonal anterograde transport together with long-range motility characteristic of anterogradely-moving PRV virions in axons (J. Scherer, I. B. Hogue, Z. A. Yaffe, N. S. Tanneti, B. Y. Winer, M. Vershinin, L. W. Enquist, submitted for publication). PRV envelope proteins, US9/gE/gI, when expressed together in neuronal cells, induced a significant decline in KIF1A protein concentration. Therefore we concluded that the viral anterograde sorting complex US9/gE/gI promotes the accelerated loss of KIF1A proteins.

This result is consistent with experiments where PC12 cells were infected with PRV strains that fail to express a functional US9/gE/gI complex to recruit KIF1A to undergo anterograde spread. These PRV mutants still promote host shutoff, leading to the decline of KIF1A proteins late in infection. However, the rate of decline is slower than that observed after wildtype PRV infection, suggesting that the US9/gE/gI complex accelerates the degradation of KIF1A by the proteasomes. The inhibition of late gene expression (e.g. US9) by AraT treatment also led to a minor yet statistically significant stabilization of KIF1A protein concentration. We concluded that the PRV anterograde sorting complex US9/gE/gI directs more KIF1A motors to be degraded by proteasomes. This might shed light on the mechanisms underlying the intrinsic instability of KIF1A protein, which potentially stem from the interaction of the motor with its cellular cargoes.

391 **PRV infection induces the accelerated loss of KIF1A protein through two separate**
392 **mechanisms.**

393

394 Our model to account for our results is shown in Figure 8. KIF1A motors, mediating the
395 anterograde transport of the vesicles in axons critical for synapse formation and function, are
396 inherently prone to proteasomal degradation. Such intrinsic instability results in the dynamic
397 steady state level of KIF1A protein maintained through rapid protein synthesis and proteasomal
398 degradation in neuronal cells (Fig. 8A). The balance between protein synthesis and degradation is
399 disrupted by PRV infection through two separate mechanisms (Fig. 8B). First, PRV infection
400 promotes the nonspecific loss of KIF1A mRNAs, and reduces the synthesis of KIF1A protein. The
401 concentration of existing KIF1A protein continues to decline through default proteasomal
402 degradation. Second, PRV infection accelerates the degradation of KIF1A protein through the
403 PRV anterograde sorting complex US9/gE/gI. We propose that US9 recruits KIF1A to transport
404 vesicles containing enveloped virions or light particles, as well as vesicles with viral glycoproteins
405 for axonal sorting and transport, and eventually this complex promotes the proteasomal
406 degradation of KIF1A in axons.

407

408 Our work implies that after reactivation from latently infected PNS neurons, the targeted loss of
409 KIF1A motor proteins leads to a limited time window for sorting into and transport of viral
410 particles in axons for further host-to-host spread. Indeed, the loss of available KIF1A motors over
411 the course of PRV infection results in reduced recruitment of the motor by US9 (14). While our
412 work has focused on PRV, it would be important to know if infection by other alphaherpesviruses
413 promotes differential degradation of axonal motor proteins. The anterograde transport of HSV-1

has been shown to be mediated by kinesin-1 (KIF5A, KIF5B, and KIF5C) and kinesin-3 (KIF1A) motors (11, 45)(E. Engel and L.W. Enquist, unpublished data). It is therefore of clinical importance to determine if HSV-1 infection induces similar loss in human neurons *in vitro*. Such a loss of kinesin-1 and kinesin-3 motors after reactivation from PNS neurson could have significant consequence for long term neuronal function. Further work is required to understand whether PNS neurons can tolerate the loss of specific kinesin motors during reactivation episodes, and whether the motor concentrations are restored after reactivation if those neurons survive.

## Materials and Methods:

**Cell lines and viruses.** Porcine kidney epithelial cells (PK15, ATCC) were maintained in Dulbecco modified Eagle medium (DMEM, Hyclone) supplemented with 10% fetal bovine serum (FBS, Hyclone) and 1% penicillin-streptomycin (Hyclone). PK15 cells were used to propagate and determine titers of all PRV strains used in this study. 293A cells (Invitrogen) were used to propagate and determine the titer of adenovirus vectors used in this study. The neuronal PC12 cell line has been used extensively to model primary neurons infection of PRV and to reproduce the US9-associated transport phenotype (14, 46). PC12 cells were cultured on dishes coated with type 1 rat tail collagen (BD Bioscience, Bedford, MA) in 85% RPMI 1640 (Thermo Fisher) supplemented with 10% horse serum(Life Technologies) and 5% FBS (47). PC12 cells were differentiated in RPMI 1640 supplemented with 1% horse serum and nerve growth factor (NGF, 2,5S, Invitrogen) at 100 ng/ml (47). Differentiation medium was replaced every third day for eight days before infection.

437 The PRV viral strains used in this study include both wild-type laboratory stain and recombinants.
438 PRV Becker is a wildtype strain (25, 26). PRV Bartha is an attenuated vaccine strain (48, 49). PRV
439 BaBe is a viral recombinant in the PRV Becker background with deletions from the unique short
440 (US) region of PRV Bartha (50). HKO146 lacks the only PRV immediate early gene IE180 and
441 expresses hSyn Cre-t2a-venus in US9 loci in the PRV Becker background (H. Oyibo, P.
442 Znamenskiy, H. V. Oviedo, L. W. Enquist, A. Zador, unpublished data). PRV161 harbors a
443 complete deletion of the US9 gene in the PRV Becker background (51). PRV172 harbors two
444 tyrosine to alanine substitutions (Y49 Y50 to AA) in the PRV Becker background (30). Individual
445 replication-deficient adenovirus vectors expressing GFP, GFP-US9, gE-mCherry, gI-mTurquoise
446 2 were previously reported (14, 52).
447
448 **Primary neuronal culture.** Embryonic superior cervical ganglia (SCG) neurons were isolated and
449 cultured as previously described (53). Briefly, superior cervical ganglia (SCG) were isolated from
450 day 17 Sprague-Dawley rat (Hilltop Labs) embryos, plated and maintained on poly-DL-ornithine
451 (Sigma-Aldrich) and laminin (Invitrogen) coated dishes (Falcon or MatTek) in neuronal medium
452 made with neurobasal medium (Gibco) supplemented with 1% penicillin-streptomycin with 2 mM
453 glutamine (Invitrogen), 2% B-27 (Gibco), and 100 ng/ml neuronal growth factor (NGF, 2.5S
454 (Invitrogen)). On two days post plating, 1 mM cytosine-D-arabinofuranoside (AraC; Sigma-
455 Aldrich) was added to selectively eliminate dividing non-neuronal cells in culture for two days.
456 SCG neurons were allowed to differentiate for at least 14 days before infection.
457
458 Compartmented neuronal cultures were prepared on poly-ornithine and laminin coated plastic
459 dishes. Parallel grooves were etched into the plastic dish, and 1% methylcellulose in neuronal

460 medium was added to the region that would underlie the middle compartment of the isolator rings.
461 CAMP320 isolator rings (Tyler Research) were coated with autoclaved silicone vacuum grease on
462 one side and gently applied to the dish so that the etched grooves extended across three
463 compartments. Dissociated SCG neurons were plated in the soma compartment (S), and were
464 allowed to extend axons along the grooves through the M compartment and into the neurite (N)
465 compartment for 14-28 days.
466
467 **Viral infection in neuronal culture.** Triplicates of differentiated PC12 cells were infected with
468 the indicated PRV strain at a multiplicity of infection (MOI) of 20 at the indicated hours post
469 infection. Infected cells from each triplicate were harvested and combined into a single sample for
470 further biochemical analysis. Compartmented SCG neuronal cultures were infected in the soma (S)
471 compartment for 24 hours. Neuronal cell bodies from the S compartments and axons from the N
472 compartments were harvested for biochemical analysis. The proteasome inhibitor MG132
473 (Millipore Sigma) was prepared in DMSO and added at a concentration of 2.5 μM. The herpesvirus
474 DNA replication inhibitor thymine 1-β-D-arabinofuranoside (AraT) (Millipore Sigma) was added
475 at a concentration of 100μg/ml 15 minutes prior to infection.
476
477 **Adenovirus vectors transduction.** The adenovirus vectors expressing GFP, GFP-US9, gE-
478 mCherry, and gI-mTurquoise-2 were reported previously (14, 52). Adenovirus vectors were
479 propagated in 293A cells, and cell-associated virus was harvested in serum-free DMEM media.
480 Adenoviral transduction of differentiated PC12 cells was performed for up to five days to ensure
481 the expression of fluorescent transgene(s) in the majority of cells (>90%).
482

**Quantitative Western blotting analysis.** Neuronal cell lysates were prepared in radioimmunoprecipitation assay buffer (RIPA) (50mM Tris-HCl, 150mM NaCl, 5mM EDTA, 1% NP-40, 0.1% SDS, 0.1% Triton X-100, and 1% sodium deoxycholate, pH 8.0) supplemented with 1 mM dithiothreitol (DTT, Sigma-Aldrich) and protease inhibitor cocktail (Sigma-Aldrich). Cell lysates were kept on ice for one hour and centrifuged at 13,200 rpm at 4°C for 10 minutes. Cleared cell lysates were transferred to a new tube and mixed with 4X LDS sample loading buffer (Invitrogen) supplemented with 240 mM DTT. The samples were heated at 95°C for 10 minutes and centrifuged at 4°C for 10 minutes to remove potential protein aggregates before proteins were separated in gradient polyacrylamide gels (4-12%) (Invitrogen). Proteins were transferred onto nitrocellulose membranes (Whatman) by semidry transfer (Bio-Rad). Membranes were blocked in 5% nonfat dry milk in Tris buffer saline with 0.1% Tween 20 (TBS-T) for 1 hour at room temperature. Primary and secondary antibodies for immunoblot analysis were prepared in 1% milk in TBS-T. Protein bands were imaged by LI-COR Odyssey CLx imaging system. The signal intensity was quantified using LI-COR Image Studio Lite software.

Antibodies used in this study included a mouse monoclonal KIF1A antibody (Clone 16, BD, at 1:2000), a mouse monoclonal kinesin heavy chain antibody (MAB-1614, Millipore Sigma, at 1:1000), a mouse monoclonal KIF3A antibody (Clone K2.4, Covance Inc., at 1:1000), a mouse monoclonal β-Actin antibody (Sigma, at 1:10000), a monoclonal US9 antibody (IA8, DSHB, at 1:100), a rabbit polyclonal GST-EP0 antibody at 1:2000 (54), a mouse monoclonal PRV VP5 antibody at 1:1000 (55), a mouse monoclonal PRV US3 antibody at 1:10000 (56), a rabbit polyclonal gE cytoplasmic tail antibody at 1:1000 (57), a rabbit polyclonal gI antibody, a generous gift from K. Bienkowska-Szewczyk, at 1:1000 (58). IRDye secondary antibodies included 800CW

donkey anti-mouse IgG, 800CW donkey anti-rabbit IgG, and 680RD donkey anti-rabbit at 1:15000 (LI-COR).

**qRT-PCR analysis.** Differentiated PC12 cells infected with PRV were harvested and subjected to total RNA extraction using an RNeasy Plus Mini Kit (Qiagen). First strand cDNA synthesis of isolated RNAs was performed with SuperScript III First Strand synthesis kit with Oligo (dT) primer (Invitrogen). Quantitative reverse transcription PCR was performed using Eppendorf Realplex$^2$ Mastercycler with reaction mixtures prepared with KAPA SYBR Fast Universal qPCR Kit (KAPA Biosystems). The PCR primers for KIF1A, KIF5B, GAPDH, and 18s rRNA were reported elsewhere (59). The qRT-PCR reaction samples were prepared in triplicates. The relative abundance of RNA in each sample was calculated using the $-\Delta\Delta C_T$ method normalized to 18s rRNA and subsequently to uninfected samples.

**Statistical analysis.** One-way analysis of variance (ANOVA) with Tukey's posttest, and two-way ANOVA with Sidak's posttest were performed using GraphPad Prism 6. Values in text, graphs, and figure legends throughout the manuscript are means ± standard errors of the means (SEM).

**Image production.**

Cartoon illustrations were made with web application BioRender under Princeton University license for education use.

**Ethics Statement.** All animal work was performed in accordance with the Princeton Institutional Animal Care and Use Committee (protocols 1947-16). Princeton personnel are required to adhere

529 to applicable federal, state, local and institutional laws and policies governing animal research,
530 including the Animal Welfare Act and Regulations (AWA); the Public Health Service Policy on
531 Humane Care and Use of Laboratory Animals; the Principles for the Utilization and Care of
532 Vertebrate Animals Used in Testing, Research and Training; and the Health Research Extension
533 Act of 1985.
534
535 **Acknowledgement**
536 We thank Halina Staniszewska-Goraczniak for excellent technical and logistical support, and the
537 rest members of the Enquist Lab for their critical comments on the projects. This project was
538 funded by NIH, National Institute of Neurological Disorders and Stroke (NINDS) RO1 NS033506
539 and RO1 NS060699 (L.W.E.).
540
541 **References**
542 1. Steiner I, Kennedy PGE, Pachner AR. 2007. The neurotropic herpes viruses: herpes
543 simplex and varicella-zoster. The Lancet Neurology 6:1015-1028.
544 2. Koelle DM, Corey L. 2008. Herpes simplex: insights on pathogenesis and possible
545 vaccines. Annu Rev Med 59:381-95.
546 3. Pomeranz LE, Reynolds AE, Hengartner CJ. 2005. Molecular biology of pseudorabies
547 virus: impact on neurovirology and veterinary medicine. Microbiol Mol Biol Rev 69:462-
548 500.
549 4. Smith G. 2012. Herpesvirus transport to the nervous system and back again. Annu Rev
550 Microbiol 66:153-76.

5. Hirokawa N, Noda Y, Tanaka Y, Niwa S. 2009. Kinesin superfamily motor proteins and intracellular transport. Nat Rev Mol Cell Biol 10:682-96.

6. Hirokawa N, Niwa S, Tanaka Y. 2010. Molecular motors in neurons: transport mechanisms and roles in brain function, development, and disease. Neuron 68:610-38.

7. Gluska S, Zahavi EE, Chein M, Gradus T, Bauer A, Finke S, Perlson E. 2014. Rabies Virus Hijacks and accelerates the p75NTR retrograde axonal transport machinery. PLoS Pathog 10:e1004348.

8. Smith GA, Pomeranz L, Gross SP, Enquist LW. 2004. Local modulation of plus-end transport targets herpesvirus entry and egress in sensory axons. Proc Natl Acad Sci U S A 101:16034-9.

9. Zaichick SV, Bohannon KP, Hughes A, Sollars PJ, Pickard GE, Smith GA. 2013. The herpesvirus VP1/2 protein is an effector of dynein-mediated capsid transport and neuroinvasion. Cell Host Microbe 13:193-203.

10. Buch A, Muller O, Ivanova L, Dohner K, Bialy D, Bosse JB, Pohlmann A, Binz A, Hegemann M, Nagel CH, Koltzenburg M, Viejo-Borbolla A, Rosenhahn B, Bauerfeind R, Sodeik B. 2017. Inner tegument proteins of Herpes Simplex Virus are sufficient for intracellular capsid motility in neurons but not for axonal targeting. PLoS Pathog 13:e1006813.

11. DuRaine G, Wisner TW, Paul Howard P, Johnson DC. 2018. Kinesin-1 Proteins KIF5A, -5B, and -5C Promote Anterograde Transport of Herpes Simplex Virus Enveloped Virions in Axons. Journal of Virology 92.

572 12. Radtke K, Kieneke D, Wolfstein A, Michael K, Steffen W, Scholz T, Karger A, Sodeik B.
573 2010. Plus- and minus-end directed microtubule motors bind simultaneously to herpes
574 simplex virus capsids using different inner tegument structures. PLoS Pathog 6:e1000991.
575 13. Wolfstein A, Nagel CH, Radtke K, Dohner K, Allan VJ, Sodeik B. 2006. The inner
576 tegument promotes herpes simplex virus capsid motility along microtubules in vitro.
577 Traffic 7:227-37.
578 14. Kramer T, Greco TM, Taylor MP, Ambrosini AE, Cristea IM, Enquist LW. 2012. Kinesin-
579 3 mediates axonal sorting and directional transport of alphaherpesvirus particles in neurons.
580 Cell Host Microbe 12:806-14.
581 15. Kratchmarov R, Kramer T, Greco TM, Taylor MP, Ch'ng TH, Cristea IM, Enquist LW.
582 2013. Glycoproteins gE and gI are required for efficient KIF1A-dependent anterograde
583 axonal transport of alphaherpesvirus particles in neurons. J Virol 87:9431-40.
584 16. Scherer J, Yaffe ZA, Vershinin M, Enquist LW. 2016. Dual-Color Herpesvirus Capsids
585 Discriminate Inoculum from Progeny and Reveal Axonal Transport Dynamics. J Virol
586 90:9997-10006.
587 17. Siddiqui N, Straube A. 2017. Intracellular Cargo Transport by Kinesin-3 Motors.
588 Biochemistry (Mosc) 82:803-815.
589 18. Kern JV, Zhang YV, Kramer S, Brenman JE, Rasse TM. 2013. The kinesin-3, unc-104
590 regulates dendrite morphogenesis and synaptic development in Drosophila. Genetics
591 195:59-72.
592 19. Klopfenstein DR, Tomishige M, Stuurman N, Vale RD. 2002. Role of
593 Phosphatidylinositol(4,5)bisphosphate Organization in Membrane Transport by the
594 Unc104 Kinesin Motor. Cell 109:347-58.

595 20. Yonekawa Y, Harada A, Okada Y, Funakoshi T, Kanai Y, Takei Y, Terada S, Noda T,
596 Hirokawa N. 1998. Defect in Synaptic Vesicle Precursor Transport and Neuronal Cell
597 Death in KIF1A Motor Protein–deficient Mice. The Journal of Cell Biology 141:431-441.
598 21. Okada Y, Yamazaki H, Sekine-Aizawa Y, Hirokawa N. 1995. The Neuron-Specific
599 Kinesin Superfamily Protein KIFIA Is a Unique Monomeric Motor for Anterograde
600 Axonal Transport of Synaptic Vesicle Precursors. Cell 81:769-780.
601 22. Kumar J, Choudhary BC, Metpally R, Zheng Q, Nonet ML, Ramanathan S, Klopfenstein
602 DR, Koushika SP. 2010. The Caenorhabditis elegans Kinesin-3 motor UNC-104/KIF1A is
603 degraded upon loss of specific binding to cargo. PLoS Genet 6:e1001200.
604 23. Smith GA, Gross SP, Enquist LW. 2001. Herpesviruses use bidirectional fast-axonal
605 transport to spread in sensory neurons. Proc Natl Acad Sci U S A 98:3466-70.
606 24. Becker Y, Tavor E, Asher Y, Berkowitz C, Moyal M. 1993. Effect of Herpes Simplex
607 Virus Type-1 UL41 Gene on the Stability of mRNA from the Cellular Genes: beta-actin,
608 Fibronectin, Glucose Transporter-l, and Docking Protein, and on Virus Intraperitoneal
609 Pathogenicity to Newborn Mice. Virus Genes 7:133-143.
610 25. Smibert CA, Johnson DC, Smiley JR. 1992. Identification and characterization of the
611 virion-induced host shutoff product of herpes simplex virus gene UL41. Journal of General
612 Virology 73:467-470.
613 26. Hardy WR, Sandri-Goldin RM. 1994. Herpes Simplex Virus Inhibits Host Cell Splicing,
614 and Regulatory Protein ICP27 Is Required for This Effect. Journal of Virology 68:7790-
615 7799.

27. Hardwicke MA, Sandri-Goldin RM. 1994. The Herpes Simplex Virus Regulatory Protein ICP27 Contributes to the Decrease in Cellular mRNA Levels during Infection. Journal of Virology 68:4797-4810.

28. Wu BW, Engel EA, Enquist LW. 2014. Characterization of a replication-incompetent pseudorabies virus mutant lacking the sole immediate early gene IE180. MBio 5:e01850.

29. Oyibo HK, Znamenskiy P, Oviedo HV, Enquist LW, Zador AM. 2014. Long-term Cre-mediated retrograde tagging of neurons using a novel recombinant pseudorabies virus. Front Neuroanat 8:86.

30. Brideau A, D., Eldridge M, Enquist LW. 2000. Directional Transneuronal Infection by Pseudorabies Virus Is Dependent on an Acidic Internalization Motif in the Us9 Cytoplasmic Tail. Journal of Virology 74:4549-4561.

31. Taylor MP, Kramer T, Lyman MG, Kratchmarov R, Enquist LW. 2012. Visualization of an alphaherpesvirus membrane protein that is essential for anterograde axonal spread of infection in neurons. MBio 3.

32. Cohen LD, Zuchman R, Sorokina O, Muller A, Dieterich DC, Armstrong JD, Ziv T, Ziv NE. 2013. Metabolic turnover of synaptic proteins: kinetics, interdependencies and implications for synaptic maintenance. PLoS One 8:e63191.

33. Hakim V, Cohen LD, Zuchman R, Ziv T, Ziv NE. 2016. The effects of proteasomal inhibition on synaptic proteostasis. EMBO J 35:2238-2262.

34. Hoogenraad CC, Feliu-Mojer MI, Spangler SA, Milstein AD, Dunah AW, Hung AY, Sheng M. 2007. Liprinalpha1 degradation by calcium/calmodulin-dependent protein kinase II regulates LAR receptor tyrosine phosphatase distribution and dendrite development. Dev Cell 12:587-602.

639 35. Schlager MA, Hoogenraad CC. 2009. Basic mechanisms for recognition and transport of
640 synaptic cargos. Mol Brain 2:25.
641 36. Kondo S, Sato-Yoshilake R, Noda Y, Aizawa H, Nakata T, Matsuura Y, Hirokawa N. 1994.
642 KIF3A Is a New Microtubule-based Anterograde Motor in the Nerve Axon. The Journal
643 of Cell Biology 125:1095-1107.
644 37. Yamazaki H, Nakata T, Okada Y, Hirokawa N. 1995. KIF3A/B: A Heterodimeric Kinesin
645 Superfamily Protein That Works as a Microtubule Plus End-directed Motor for Membrane
646 Organelle Transport. The Journal of Cell Biology 130:1387-1399.
647 38. Li J-Y, Pfister KK, Brady S, Dahlstrom A. 1999. Axonal Transport and Distribution of
648 Immunologically Distinct Kinesin Heavy Chains in Rat Neurons. Journal of Neuroscience
649 Research 58.
650 39. Hirokawa N, SatoYoshitake R, Kobayashi N, Pfister KK, Bloom GS, Brady ST. 1991.
651 Kinesin Associates with Anterogradely Transported Membranous Organelles In Vivo. The
652 Journal of Cell Biology, 114:295-302.
653 40. Everly DN, Jr., Feng P, Mian IS, Read GS. 2002. mRNA degradation by the virion host
654 shutoff (Vhs) protein of herpes simplex virus: genetic and biochemical evidence that Vhs
655 is a nuclease. J Virol 76:8560-71.
656 41. Perez-Parada J, Saffran HA, Smiley JR. 2004. RNA degradation induced by the herpes
657 simplex virus vhs protein proceeds 5' to 3' in vitro. J Virol 78:13391-4.
658 42. Taddeo B, Roizman B. 2006. The virion host shutoff protein (UL41) of herpes simplex
659 virus 1 is an endoribonuclease with a substrate specificity similar to that of RNase A. J
660 Virol 80:9341-5.

661 43. Doepker RC, Hsu WL, Saffran HA, Smiley JR. 2004. Herpes simplex virus virion host
662 shutoff protein is stimulated by translation initiation factors eIF4B and eIF4H. J Virol
663 78:4684-99.
664 44. Feng P, Everly DN, Jr., Read GS. 2005. mRNA decay during herpes simplex virus (HSV)
665 infections: protein-protein interactions involving the HSV virion host shutoff protein and
666 translation factors eIF4H and eIF4A. J Virol 79:9651-64.
667 45. Diefenbach RJ, Davis A, Miranda-Saksena M, Fernandez MA, Kelly BJ, Jones CA, LaVail
668 JH, Xue J, Lai J, Cunningham AL. 2016. The Basic Domain of Herpes Simplex Virus 1
669 pUS9 Recruits Kinesin-1 To Facilitate Egress from Neurons. J Virol 90:2102-11.
670 46. Lyman MG, Curanovic D, Enquist LW. 2008. Targeting of pseudorabies virus structural
671 proteins to axons requires association of the viral Us9 protein with lipid rafts. PLoS Pathog
672 4:e1000065.
673 47. Ch'ng TH, Flood EA, Enquist LW. 2005. Culturing Primary and Transformed Neuronal
674 Cells for Studying Pseudorabies Virus Infection. Methods Mol Biol 292:299-316.
675 48. Platt KB, Mare CJ, Hinz PN. 1979. Differentiation of Vaecine Strains and Field Isolates of
676 Pseudorabies (Aujeszky's Disease) Virus: Thermal Sensitivity and Rabbit Virulence
677 Markers. Archives of Virology 60:13-23.
678 49. Szpara ML, Tafuri YR, Parsons L, Shamim SR, Verstrepen KJ, Legendre M, Enquist LW.
679 2011. A wide extent of inter-strain diversity in virulent and vaccine strains of
680 alphaherpesviruses. PLoS Pathog 7:e1002282.
681 50. Card JP, Whealy ME, Robbins AK, Enquist LW. 1992. Pseudorabies Virus Envelope
682 Glycoprotein gI Influences both Neurotropism and Virulence during Infection of the Rat
683 Visual System. Journal of Virology 66:3032-3041.

684 51. Brideau AD, Card JP, Enquist LW. 2000. Role of pseudorabies virus Us9, a type II
685 membrane protein, in infection of tissue culture cells and the rat nervous system. J Virol
686 74:834-45.
687 52. Hogue IB, Scherer J, Enquist LW. 2016. Exocytosis of Alphaherpesvirus Virions, Light
688 Particles, and Glycoproteins Uses Constitutive Secretory Mechanisms. MBio 7.
689 53. Curanovic D, Ch'ng TH, Szpara M, Enquist L. 2009. Compartmented neuron cultures for
690 directional infection by alpha herpesviruses. Curr Protoc Cell Biol Chapter 26:Unit 26 4.
691 54. Brukman A, Enquist LW. 2006. Pseudorabies virus EP0 protein counteracts an interferon-
692 induced antiviral state in a species-specific manner. J Virol 80:10871-3.
693 55. Lyman MG, Feierbach B, Curanovic D, Bisher M, Enquist LW. 2007. Pseudorabies virus
694 Us9 directs axonal sorting of viral capsids. J Virol 81:11363-71.
695 56. Olsen LM, Ch'ng TH, Card JP, Enquist LW. 2006. Role of pseudorabies virus Us3 protein
696 kinase during neuronal infection. J Virol 80:6387-98.
697 57. Tirabassi RS, Enquist LW. 2000. Role of the Pseudorabies Virus gI Cytoplasmic Domain
698 in Neuroinvasion, Virulence, and Posttranslational N-Linked Glycosylation. Journal of
699 Virology 74:3505–3516.
700 58. Tirabassi RS, Enquist LW. 1998. Role of Envelope Protein gE Endocytosis in the
701 Pseudorabies Virus Life Cycle. Journal of Virology 72:4571–4579.
702 59. Baptista FI, Pinto MJ, Elvas F, Almeida RD, Ambrosio AF. 2013. Diabetes alters KIF1A
703 and KIF5B motor proteins in the hippocampus. PLoS One 8:e65515.

704 **Figure legends**

705 **Fig. 1. KIF1A protein undergoes rapid accumulation and degradation in neuronal cells upon**
706 **MG132 and CHX treatments.**

(A) Differentiated PC12 cells were treated with the translation inhibitor cycloheximide, proteasome inhibitor MG132, or both cycloheximide and MG132 for 2, 4, 6, 8, hours. Cells were harvested at indicated time points and lysates were analyzed by Western blot to monitor protein levels of KIF1A, KIF5, KIF3A, and actin. (B-D) KIF1A, KIF5, and KIF3A protein levels were measured by band intensities and normalized to actin protein levels for each time interval. Normalized values were again normalized to that of Mock 0 hour samples. Values are means plus SEMs (error bar) from three independent experiments. n.s., not statistically significant, **, P<0.01, ***, P<0.001, ****, P<0.0001 for the indicated comparison at 8 hours post treatment.

**Fig. 2. KIF1A protein concentration is reduced during PRV infection in neuronal cells.**

(A and B) Differentiated PC12 cells were mock-infected or infected with PRV Becker for 3, 8, 12, 16, 20, 24 hours with MOI of 20. Cells were harvested at the time intervals shown, and lysates were analyzed by Western blot to monitor protein levels of KIF1A, KIF5, KIF3A, and actin. Kinesin levels were measured by band intensities and normalized with respect to actin levels at each time interval. Normalized values were again normalized to that of Mock 0 hour samples. Values are means plus SEMs (error bars) from four independent experiments. n.s., not statistically significant, ***, P<0.001, ****, P<0.0001.

**Fig. 3. The abundance of KIF1A, KIF5B, and GAPDH transcripts is significantly reduced in PRV-infected neuronal cells.**

Differentiated PC12 cells were infected with (A) PRV Becker or (B) PRV Bartha for 3, 8, 12, 16, 20, 24 hours with MOI of 20. Cells were harvested at the time intervals shown. Total RNA were extracted and qRT-PCR quantification was performed to measure KIF1A, KIF5B, and GAPDH

mRNA levels using 18S rRNA as internal control at each time interval. The normalized values are then normalized to that of Mock 0 hour samples. Values are means plus SEMs (error bars) from three independent experiments.

**Fig. 4. KIF1A is degraded by the proteasome in the late phase of PRV infection.**

Differentiated PC12 cells were (A) mock-infected or (B) infected with PRV Becker for 8, 12, 16, 20, 24 hours with MOI of 20. In a parallel experiment, the proteasomal inhibitor, MG132, was added at 12 hours post infection at the concentration of 2.5 μM. KIF1A levels were analyzed by Western blot and normalized to actin levels at each time interval. Normalized values were again normalized to that of Mock 0 hour samples. Values are means plus SEMs (error bars) from three independent experiments. **, P<0.01 for comparison between PRV-infected and PRV-infected+MG132 samples.

**Fig. 5. PRV infection of compartmented primary neuronal cultures leads to reduction of KIF1A protein and proteasomal degradation in axons.**

(A) Illustration of *in vitro* culture of primary superior cervical ganglion neurons using modified Campenot chambers that include the S (soma), M (methocel), and N (neurite, axon termini) compartments. 10^6 PFU of PRV Becker was added in the S (soma) compartment. (B and C) SCG neurons were infected at the Soma (S) compartment with PRV Becker for 24 hours. (B) Cell bodies and axons from S and N compartments were collected at the time intervals show, and lysate were analyzed by Western blot to monitor the levels of KIF1A and Actin. (C) DMSO or MG132 (2.5 μM) were added to the N (Neurite) compartment at 8 hpi. Cell bodies and axons from S and N

compartments were collected at the time intervals show, and lysate were analyzed by Western blot to monitor the levels of KIF1A and Actin.

**Fig. 6. Accelerated proteasomal degradation of KIF1A during infection requires the expression of both PRV early and late proteins**.

(A) *De novo* PRV viral protein synthesis is required for KIF1A degradation. Differentiated PC12 cells were mock-infected or infected with PRV Becker, UV'd PRV Becker, or IE180-null PRV (HKO146) for 24 hours with MOI of 20. Cells were harvested and lysates were analyzed by Western blot to monitor the levels of KIF1A, actin, and VP5 at indicated time intervals. (B) Differentiated PC12 cells were mock-treated or treated with AraT (100μg/ml) starting 15 minutes before being infected with PRV Becker for 0, 8, 12, 16, 20, 24 hours. Samples were collected at the indicated time intervals. Lysates were subjected to Western Blot analysis to measure protein levels of KIF1A, actin, VP5, and EP0. (C) For every infection, KIF1A protein abundance were measured by band intensities and normalized with respect to actin levels at each time interval. Normalized values were then normalized to that for Mock 0 hour samples. Values are means plus SEMs (error bars) from three independent experiments. *, $P<0.05$ for PRV Becker vs. PRV Becker with AraT comparison at specified time interval.

**Fig. 7. PRV anterograde-spread complex US9/gE/gI promotes the accerlated degradation of KIF1A proteins.**

(A) Differentiated PC12 cells were infected with PRV Becker, or different PRV mutants defective in anterograde spread (results from PRV BaBe and PRV161 infections are shown) for 0, 8, 12, 16, 20 ,24 hours. Cells were harvested and lysates were analyzed by Western blot to monitor KIF1A

775 and actin protein Level. (B) For every infection, KIF1A levels were measured by band intensities
776 and normalized with respect to actin levels at each time interval. Normalized values were then
777 normalized to that for Mock 0 hour samples. Values are means plus SEMs (error bars) from seven
778 independent experiments. *, $P<0.05$ for all mutants vs. PRV Becker at specified time interval. (C)
779 Differentiated PC12 cells were transduced with Adenoviral vectors expressing GFP, GFP-US9, or
780 GFP-US9/gE-mCherry/gI-mTurquoise 2. Cells were collected at indicated days post transduction
781 (d.p.t.) and subjected to Western Blot Analysis to monitor KIF1A and Actin level.
782
783 **Fig. 8. PRV infection induces the accelerated loss of KIF1A protein through two separate**
784 **mechanisms.**
785 (A) In uninfected cells, KIF1A protein is inherently prone to be degraded by the proteasome. The
786 steady state concentration of KIF1A protein is achieved through rapid protein synthesis and
787 proteasomal degradation. (B) PRV infection induces KIF1A mRNA degradation and reduced
788 protein synthesis, while the existing KIF1A proteins undergo default proteasomal degradation.
789 Furthermore, the proteasomal degradation of the existing KIF1A proteins is accelerated by the
790 PRV gE/gI/US9 complex in the late phase of infection. Images were created with BioRender.
791

# Figure 1

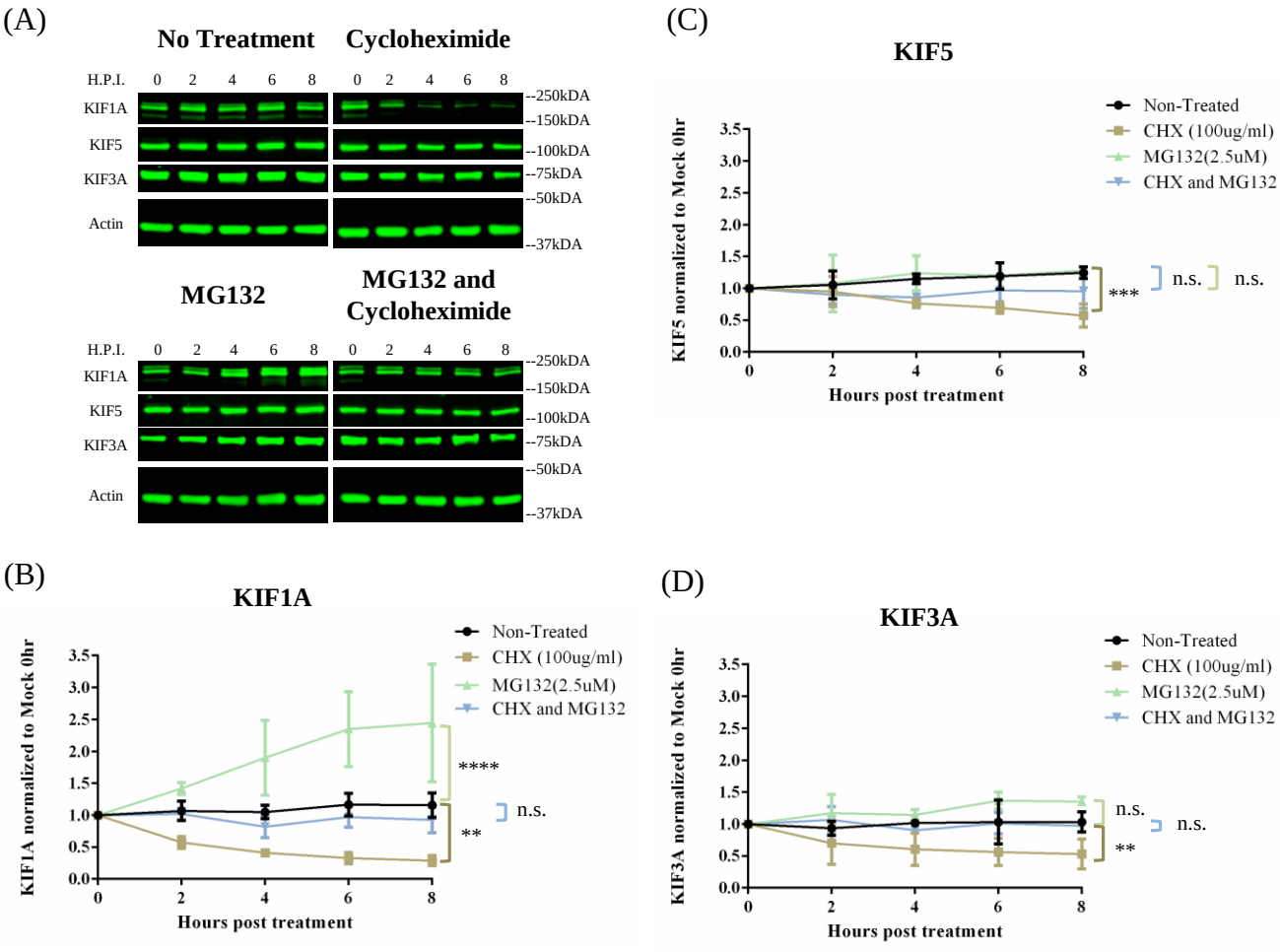


Fig. 1. KIF1A protein undergoes rapid accumulation and degradation in neuronal cells upon MG132 and CHX treatments.

# Figure 2

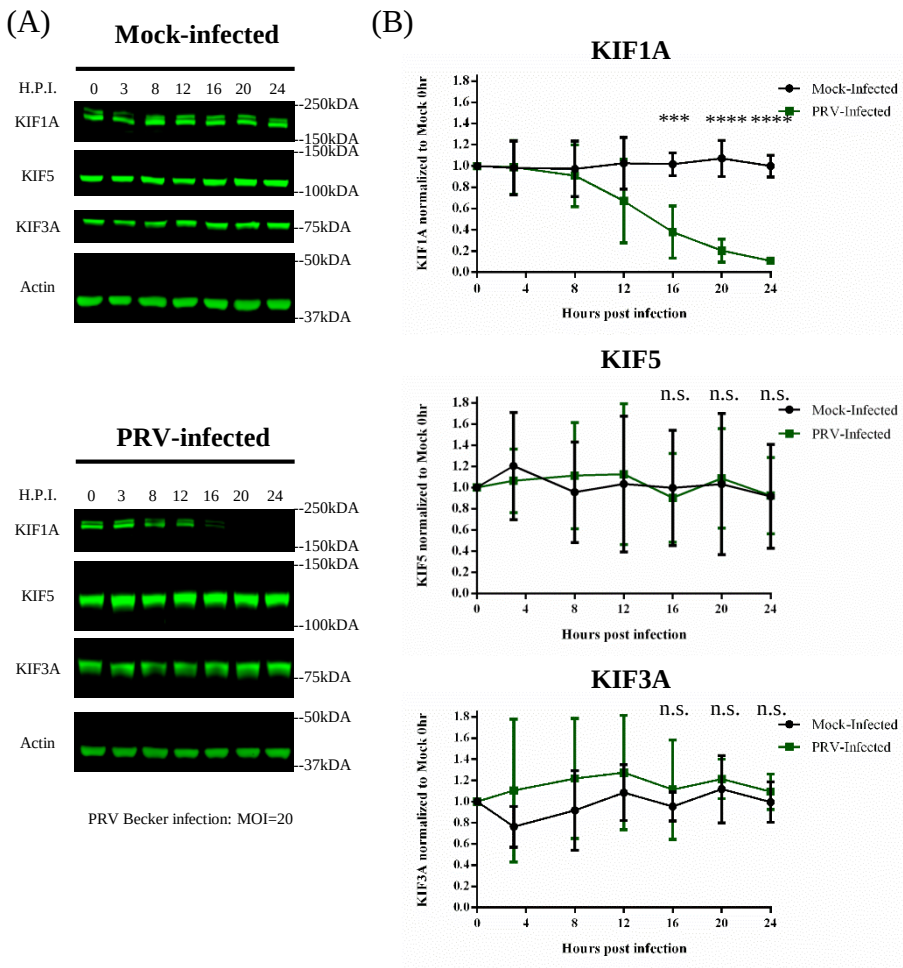


Fig. 2. KIF1A protein concentration is reduced during PRV infection in neuronal cells.

# Figure 3

(A) (B)

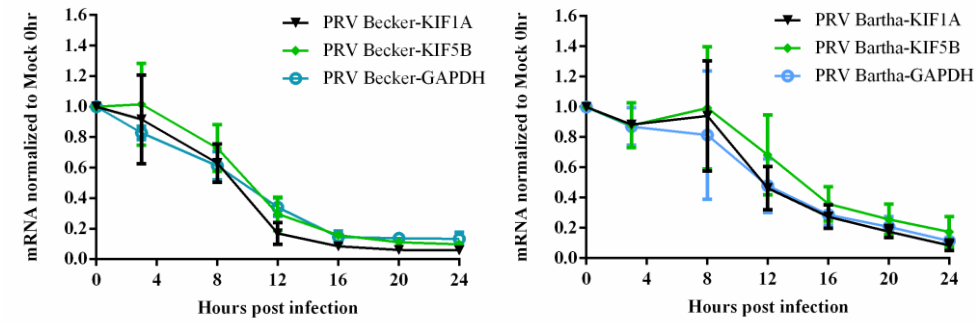


Fig. 3. The abundance of KIF1A, KIF5B, and GAPDH transcripts is significantly reduced in PRV-infected neuronal cells.

# Figure 4

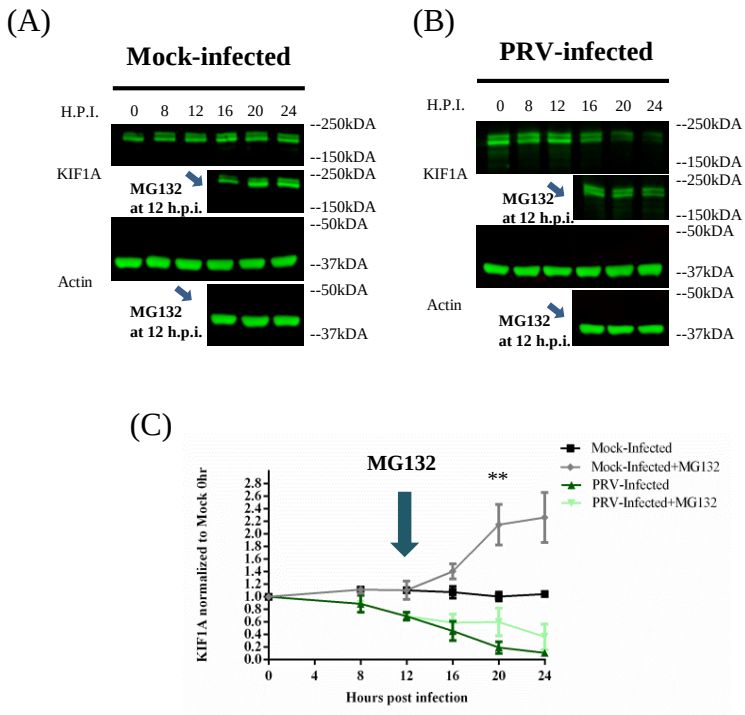


Fig. 4. KIF1A is degraded by the proteasome in the late phase of PRV infection.

# Figure 5

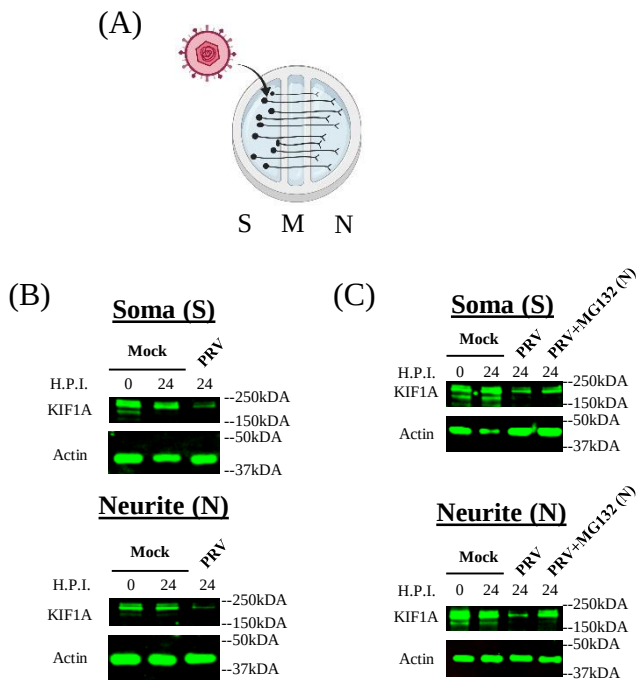


Fig. 5. PRV infection of compartmented primary neuronal cultures leads to reduction of KIF1A protein and proteasomal degradation in axons.

# Figure 6

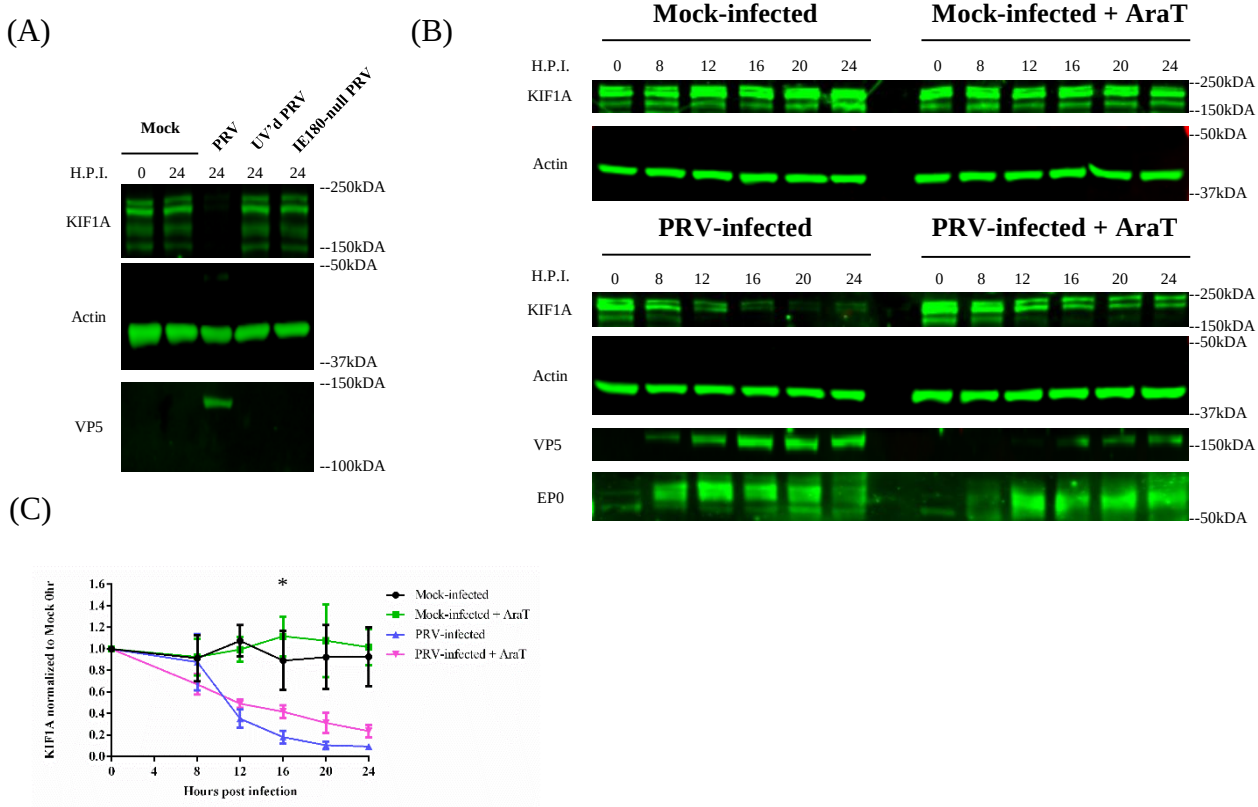


Fig. 6. Accelerated proteasomal degradation of KIF1A during infection requires the expression of both PRV early and late proteins.

# Figure 7

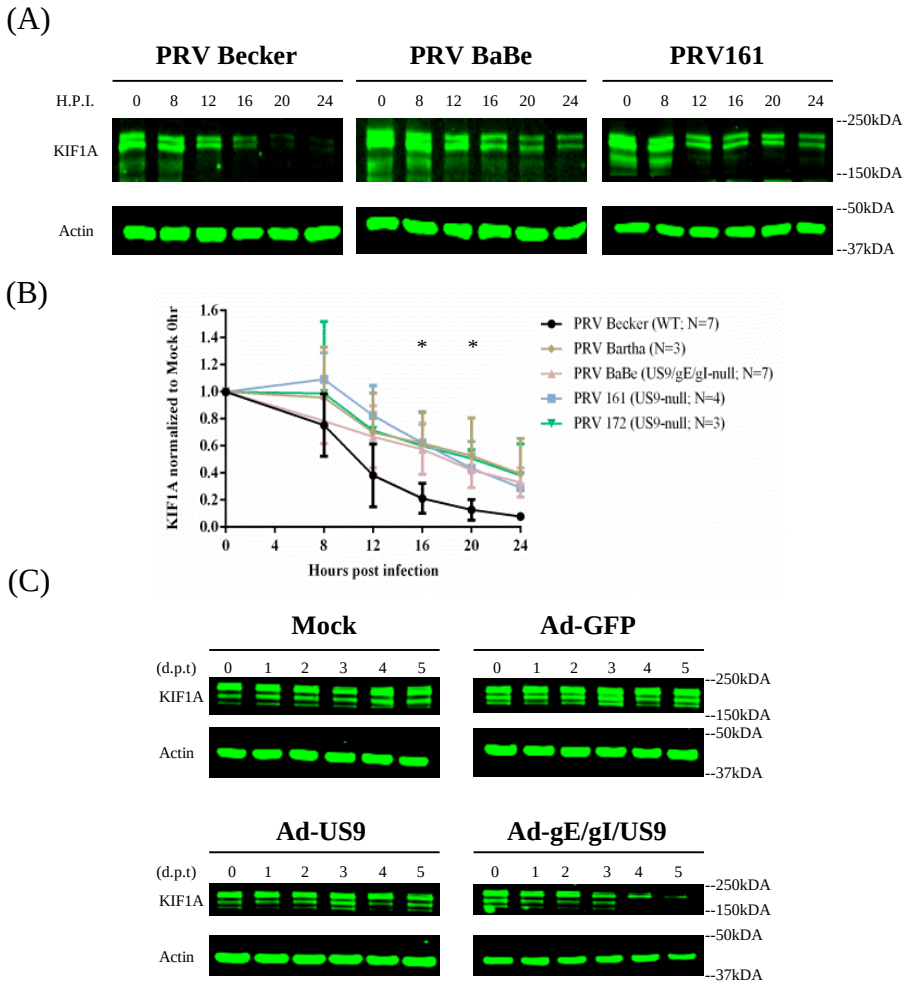


Fig. 7. PRV anterograde-spread complex US9/gE/gI promotes the accelerated degradation of KIF1A proteins.

# Figure 8 (MODEL)

(A)

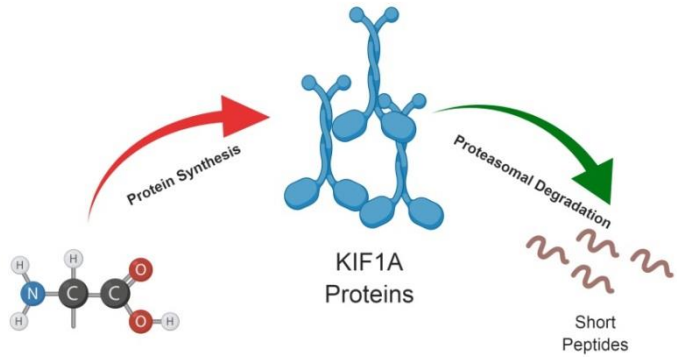


(B)

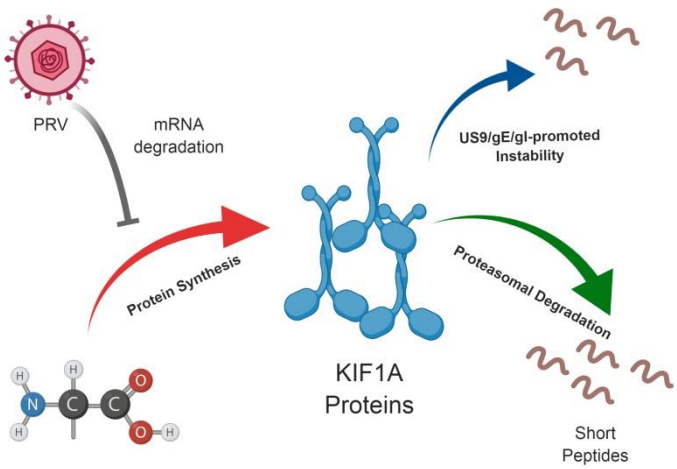


Fig. 8. PRV infection induces the accelerated loss of KIF1A protein through two separate mechanisms.

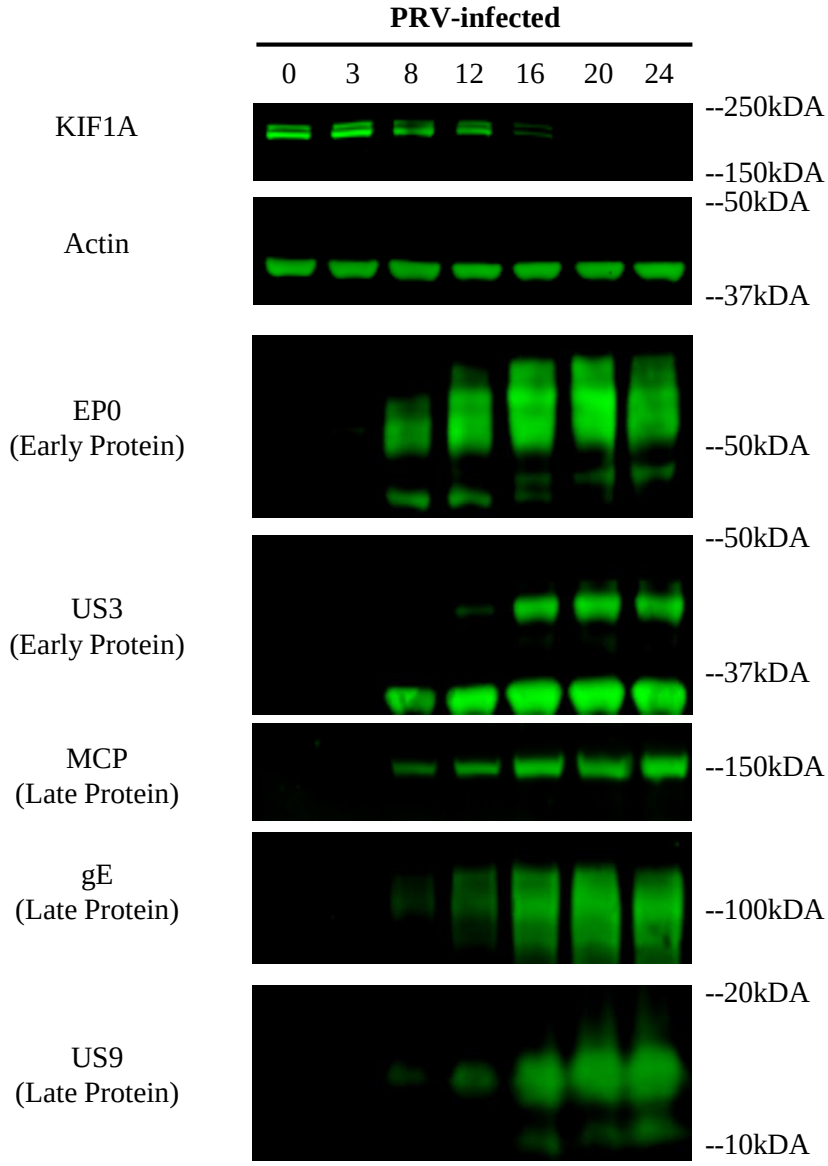


Figure S1. PRV early and late gene expressions in differentiated PC12 cells.

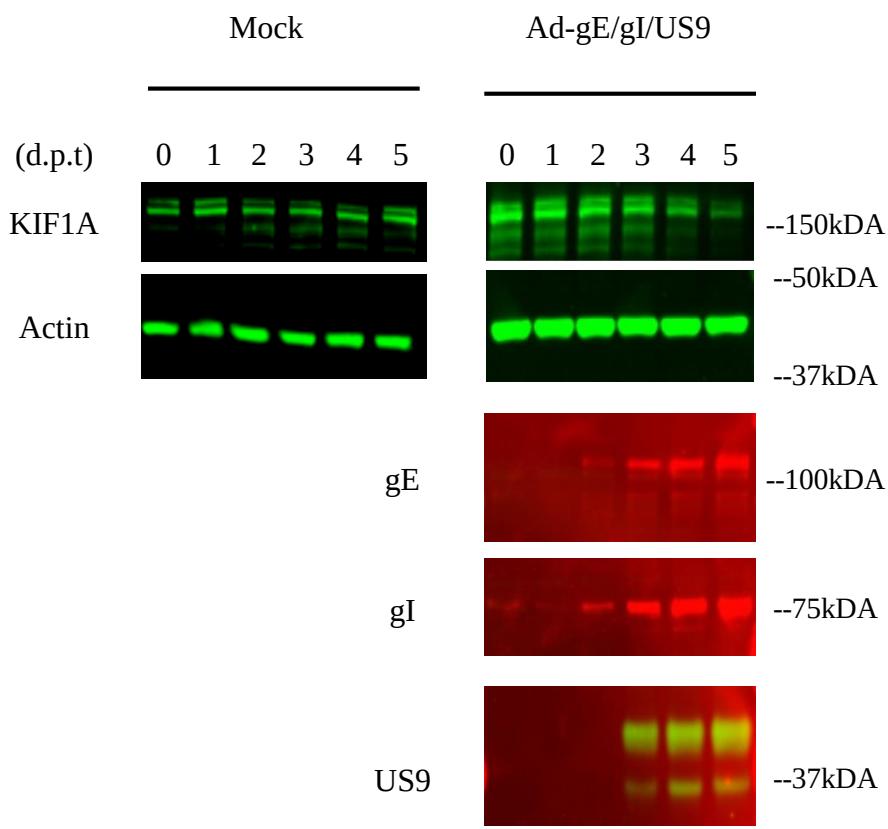


**Figure S2. Expression of transduced genes US9, gE, and gI in differentiated PC12 cells.**